DFIG (Doubly-Fed Induction Generator) control for wind turbines

TN156 | Posted on June 5, 2024 | Updated on May 7, 2025

Dhruv KANSARA
Sales & Development Engineer
imperix

Table of Contents

This technical note demonstrates the control of a Doubly-Fed Induction Generator (DFIG) in a wind turbine application. Firstly, the operating principles and control strategy for a grid-tied DFIG are discussed. A 2MW DFIG is then modeled in an RT-Box to demonstrate how the B-Box RCP can be used in conjunction with a HIL simulator to control complex systems.

DFIG versus SCIM for wind turbine applications

The doubly-fed induction generator (DFIG) is an improvement over its predecessor, the squirrel cage induction machine (SCIM), for generator use cases. It is particularly

suitable for cases where the generator speed and torque must be flexible, such as wind turbines.

By comparing the SCIM to the DFIG, the overall benefit of selecting the DFIG can be further analyzed.

Since the slip is not controllable in SCIMs, there are a couple of methods to maximize the generated power in a SCIM-based wind turbine:

- control the rotor using only the blade pitch (slow) and a gearbox given that the SCIM is grid-connected;
- utilize a variable frequency drive to control the stator voltage and process 100% of the generated power through the converter.

On the other hand, as the DFIG has accessible rotor windings, slip can be controlled by controlling the rotor currents, and the slip is no longer dependent on the turbine operating conditions. As a result of the accessible rotor windings, the DFIG can be controlled using the topology shown in Figure 1 [1].

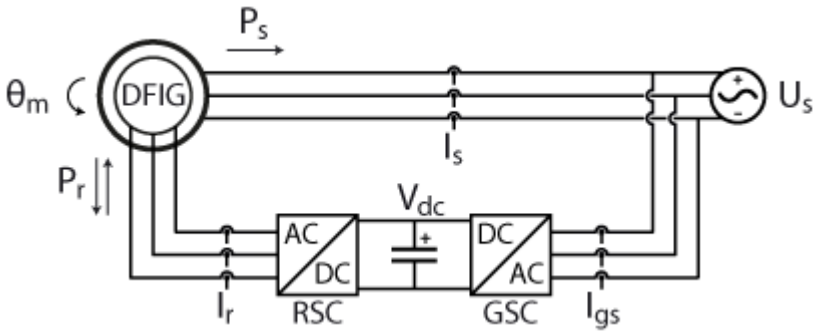

Figure 1: Simplified topology of grid-tied DFIG, popular in wind turbine applications

The topology shown in Figure 1 possesses the following additional advantages:

- assuming small values of slip, the rotor power, and therefore the converter power rating, is a small percentage of the total generated power;
- fluctuations in wind speed can be dealt with using fast rotor current control, bypassing the need for a comparatively inefficient multi-ratio gearbox;
- the controllable slip allows performing MPPT for maximum power generation electrically instead of mechanically.

The control of the grid-side converter (GSC), and the rotor-side converter (RSC) in Figure 1 is discussed in detail in section 3 of this article.

DFIG operating principle

The rotor speed in a DFIG, operated according to the topology shown in Figure 1, is controlled using the rotor current. Similarly to the induced rotor currents in a SCIM, the rotor currents in the DFIG are synchronized to the slip angle θ_{slip}. Therefore, the control of the rotor currents can be done by orienting the control to ω_{slip}. [1]

$$\omega_{slip} = \omega_{stator} - p\,\omega_m$$

Since the rotor currents can be manipulated by the RSC, increasing or decreasing rotor current allows for the control of the rotor magnetic field strength. This manipulation allows the DFIG to change the speed of the rotor with respect to the stator frequency. As referred to before, this ratio is referred to as slip and can be calculated in the following manner : [1]

$$s = \frac{\omega_{slip}}{\omega_{stator}}$$

Since the rotor speed can be changed using the rotor current, the DFIG can operate both subsynchronously and hypersynchronously. Figure 2 illustrates the two modes of operation and whether the rotor is consuming or generating active power depending on the mode of operation. [1]

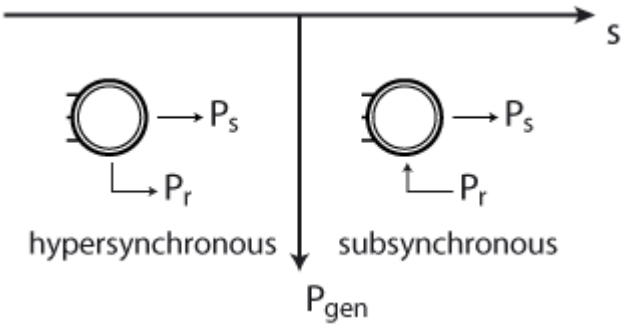

Figure 2: Rotor power direction as a function of slip in the generator quadrants of the DFIG

Following that, the stator power in a DFIG is a function of the applied mechanical power and the slip of the generator.

$$P_s = \frac{P_m}{1 - s}$$

Additionally, the power split between the rotor and stator of the DFIG is also a function of slip,

$$P_r = -sP_s,$$

hence the requirement of limiting the value of slip to remain within the rated specifications of the rotor speed controller.

DFIG power versus rotor speed

A wind turbine has a torque characteristic which is a function of the windspeed and the rotor speed. Therefore, there is an optimum rotor speed setpoint for a given wind speed. In order to model these effects, a rotor speed/torque look-up table was implemented for this article.

Figure 15 shows the rotor and stator power vary according to the rotor speed/slip for the assumed windspeed. The peak mechanical power is generated at 180 rad/s.

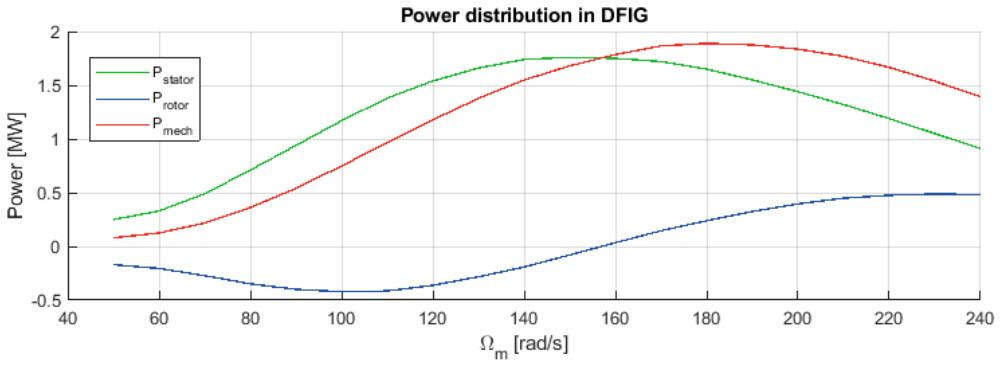

Figure 15: An example of the power distribution for a DFIG given certain wind conditions for a given rotor speed

Furthermore, Figure 16 shows that, with the applied torque profile, the (absolute) RSC power remains below 30% of full-scale power and that the DFIG can operate subsynchronously and hypersynchronously.

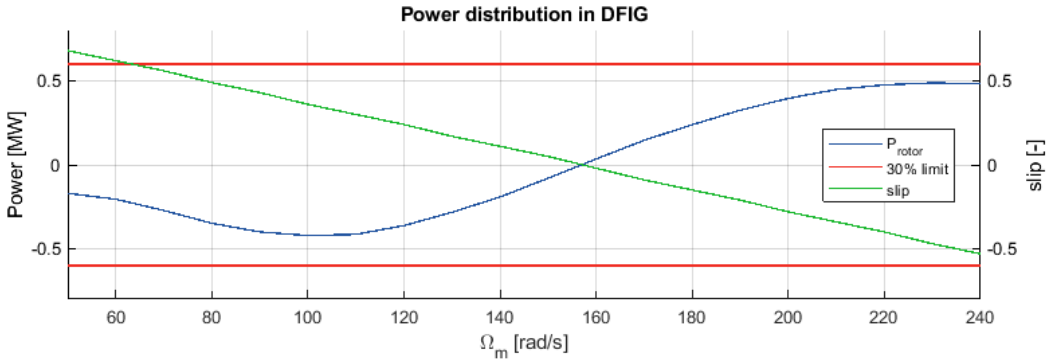

Figure 16: Rotor power and slip as a function of rotor speed in a DFIG

Control implementation for DFIG in wind turbine applications

The following sections discuss specific parts of the overall control (Figure 7) in further detail.

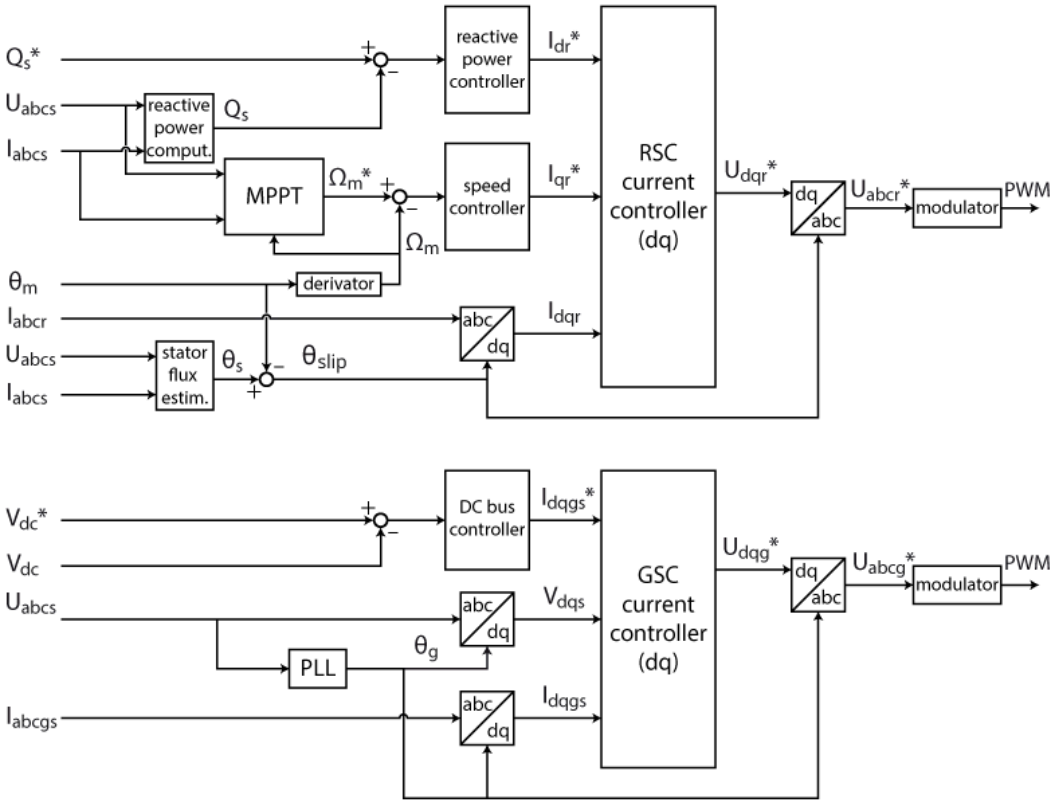

Figure 7: The overall control scheme for the RSC and the GSC for wind turbine DFIG applications

Control of the GSC

The GSC in a DFIG drive is analogous to an active front-end (AFE). It minimizes the reactive power consumed/generated by the rotor and ensures the DC bus voltage is high enough to allow for the RSC to function. Given that, Figure 3 shows the control of an AFE.

TN166 – Active Front End elaborates further on the control scheme implemented for this converter.

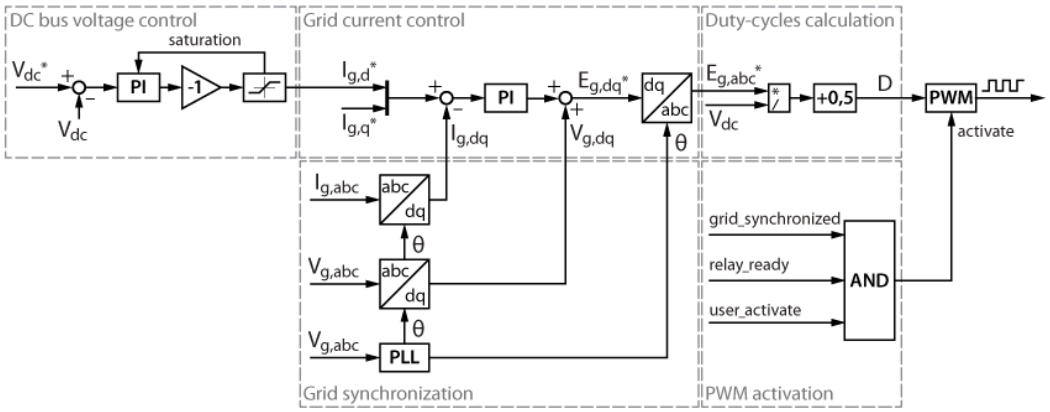

Figure 3: High-level control strategy for the active front-end

Control of the RSC

The goal of the RSC is to manipulate the rotor field in order to control the DFIG, similar to TN139 – Rotor Field-Oriented Control (RFOC) of an induction machine. The key difference is that the rotor field in a DFIG can be directly controlled, whereas in a SCIM, the rotor flux is controlled indirectly through stator currents.

Independent power control of a DFIG, connected as shown in Figure 1, is achievable because the active and reactive powers have the following relationship with the rotor current: [1]

$$P = -\frac{3}{2}\frac{L_m}{L_s}\hat{U}_g(1-s)I_{qr}$$

$$Q = \frac{3}{2}\frac{\hat{U}_g}{L_s}\left(\frac{\hat{U}_g}{\omega_s} - L_m I_{dr}\right)$$

Note that, as mentioned in the previous section, the slip is controlled indirectly by changing the applied torque on the rotor (and therefore its speed)

Inner current loop

To measure/calculate I_{qr} and I_{dr}, the RSC voltages and currents must be transformed into the slip-oriented reference frame. This is done by performing a Park transform on the measured values. The reference frame is synchronized with $\theta_{slip} = \theta_{stator} - \theta_m$. While θ_{stator} can be measured using a PLL on the grid voltage, θ_m must either be physically measured, or estimated using an observer.

Since the rotor windings may have a different number of turns compared to the stator, all values are referred to the stator, considering the transformation ratio u.

Having calculated I_{dqr}, the rotor currents can then be controlled using PI controllers (shown in Figure 4).

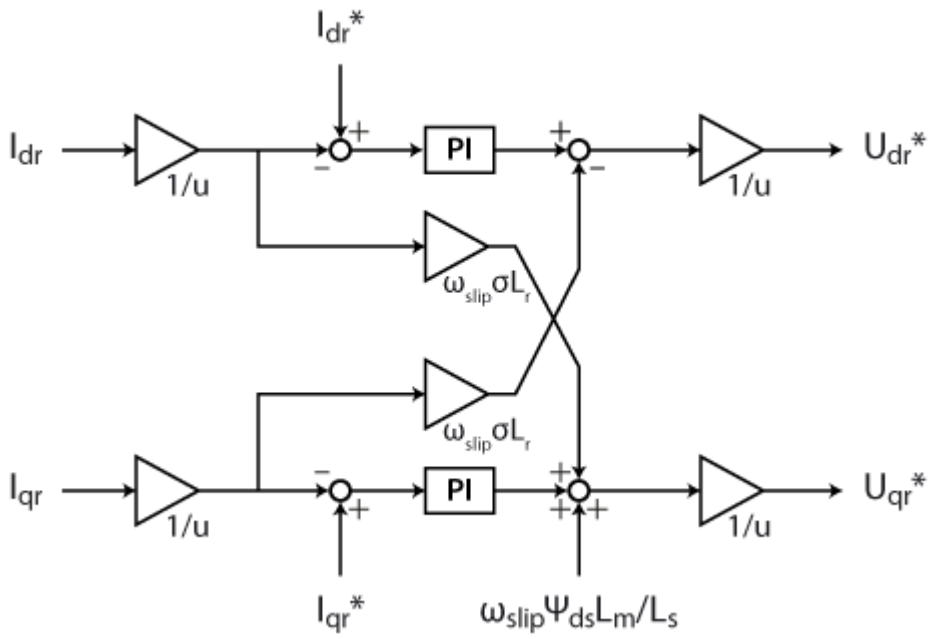

Figure 4: Rotor current control algorithm including the decoupling feedforward terms

Similarly to the RFOC of SQIM, the transient performance of the PI current controllers in Figure 4 can be improved by including I_{qr} and I_{dr} decoupling terms. As a result, the decoupling feedforward terms of the DFIG are shown in Figure 4 [1].

In the case of the DFIG, the decoupling impedance is defined as $\omega_{slip}\sigma L_r$ since the inductance that links U_{dqr} and I_{dqr} is σL_r and the frequency of the rotor currents is ω_{slip}.

Additionally, the machine equations developed in the slip reference frame exhibit a disturbance term on the q-axis. The additional decoupling term for U_{qr} [1] will further improve the transient performance of the controller.

DFIG active power control

While the active power can be directly controlled using I_{qr}, it does not make sense within the constraints of the wind turbine application. As the goal of the wind turbine is to maximize the generated power, an MPPT algorithm, such as Perturb & Observe, is more applicable for this use case (more details can be found in TN117 – Maximum Power Point Tracking (MPPT) algorithms).

In addition, given that a wind turbine is a physical system, with physical constraints on the maximum allowable rotor speed, it is desirable to have an intermediary speed controller to impose the over-speed limit for the rotor. The MPPT algorithm then acts on the speed reference instead of the I_{qr} reference, as illustrated in Figure 5.

Note that the rate limit for the speed reference is present to maintain speed variations within reasonable values, given the generator power.

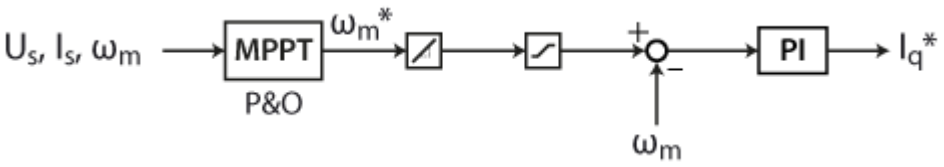

Figure 5: DFIG MPPT controller cascaded with speed controller

DFIG reactive power control

According to the equation for reactive power from section 3.2, the reactive power of the DFIG could be controlled only using feedforward control. Nevertheless, a PI controller was chosen (Figure 6) in order to compensate for any non-idealities that may be present.

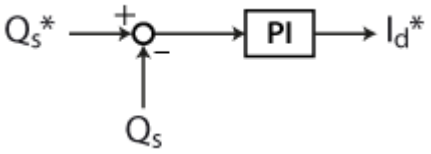

Figure 6: DFIG reactive power is controlled using a PI controller

Control validation using HIL simulation

DFIGs in wind turbines are great candidates for HIL since:

- DFIGs are usually MW-level machines that are both challenging to procure and test;
- Downscaled DFIGs are also rare and generally expensive;
- The overall system (including the wind turbine) provides an even greater challenge to perform a lab-scale test.

Modeling the DFIG on a HIL simulator

The plant was modeled in an RT-box 1 for this example. Details of the model can be found in the table below:

P_{rated} DFIG	2 MW
pole pairs	2
R_{stator}	2.2 mΩ
L_{s_stator}	0.12 mH
R_{rotor}	1.8 mΩ

L_{s_rotor}	0.05 mH
L_m	2.9 mH
Friction coefficient	0.000015
u	0.54

Table 1: DFIG parameters

P_{rated} RSC/GSC	500 kW
V_{g_LL}	690 V
V_{DC_bus}	1.5 kV
f_g	50 Hz
C_{bus}	53 mF
L_{phase}	500 µH
L_{esr}	1 mΩ

Table 2: GSC/RSC parameters

Note that the machine parameters in Tables 1 and 2 are referred from [2]. To simplify the model, the following approximations were made:

- a torque LUT is used to emulate the torque/speed characteristic of a wind turbine
- the blades of the system are lumped into a single rotational inertia
- The rotational inertia of the system is reduced to decrease the time constants of the system.

Following these approximations, a time-step of 6 µs was implemented to maximize the available resources on the HIL simulator. The plant subsequently implemented in PLECS is shown in Figure 8.

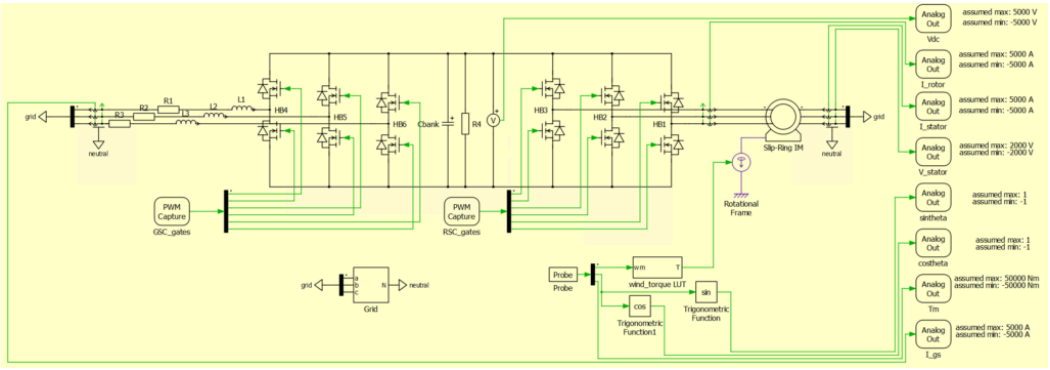

Figure 8: DFIG plant model implemented in PLECS

Implementing DFIG control on the B-Box RCP

Implementing the control is trivial using the ACG SDK and Plexim PLECS. A screenshot of the control, which can be downloaded below, is shown in Figure 9.

The control frequency selected is 20 kHz, which still makes sense given the step size of 6 µs for the plant model.

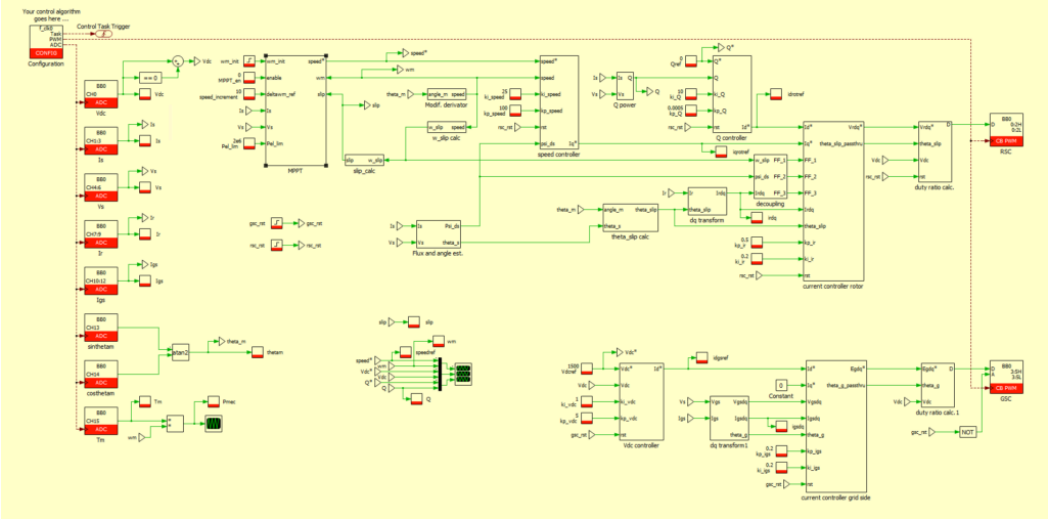

Figure 9: The control from Figure 7 implemented using PLECS

TN156_DFIG_PLECS_RTBOXDownload TN156 PLECS model

Interfacing the B-Box RCP to the HIL simulator

In order to interface the B-Box RCP to the RT-Box 1, the HIL interface needs to be used. It can be connected as seen in Figure 10 below:

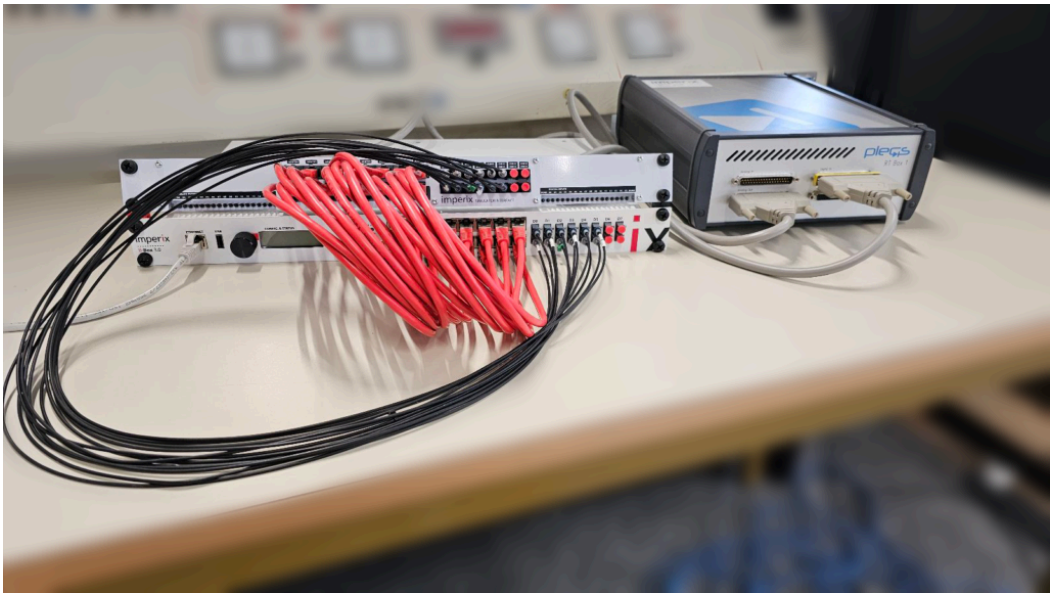

Figure 10: The HIL simulator requires an interface to send and receive signals to the B-Box RCP controller

Since the HIL simulator and the B-Box RCP only accept analog signals between +10 V and -10 V, the signals must be scaled within these limits, as shown in Figures 11 and 12. Likewise, Figures 13 and 14 illustrate how to set the PWM capture block to accept the PWM outputs from the B-Box RCP.

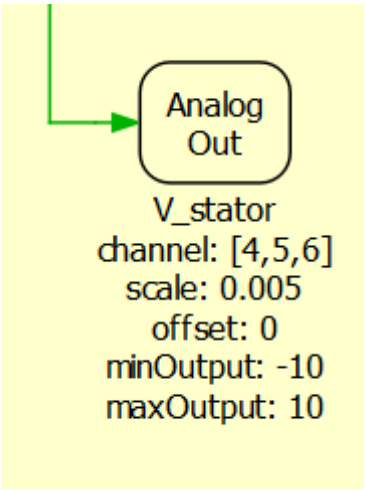

Figure 11: Analog out block

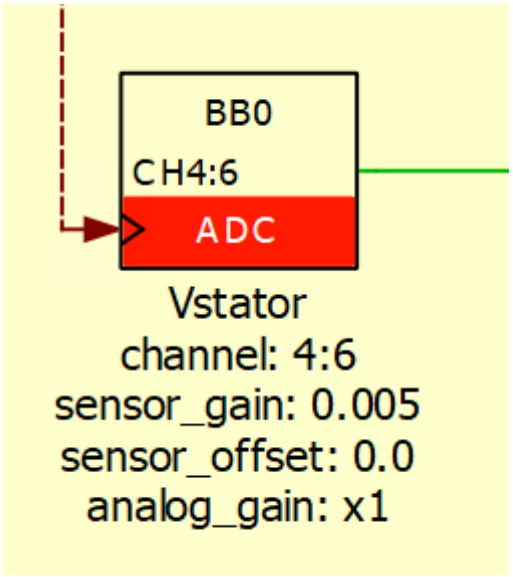

Figure 12: ADC block

Setting the scale in Figure 11 and the sensitivity in Figure 12 to the same value (assuming a gain of 1) ensures that the controller inputs are correctly scaled

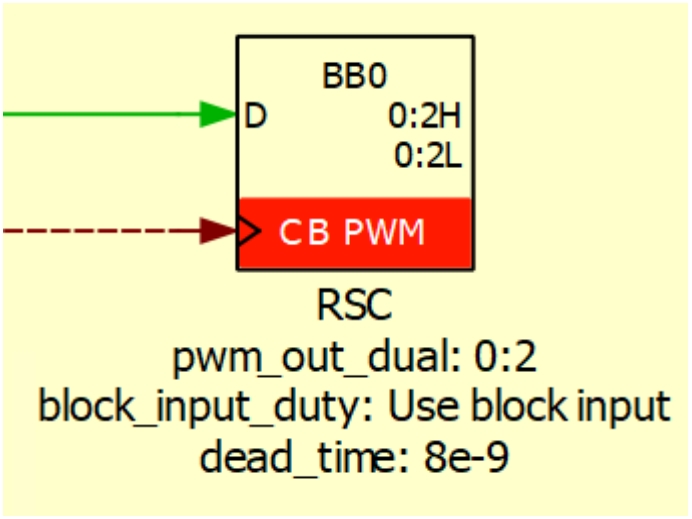

Figure 13: PWM modulator block

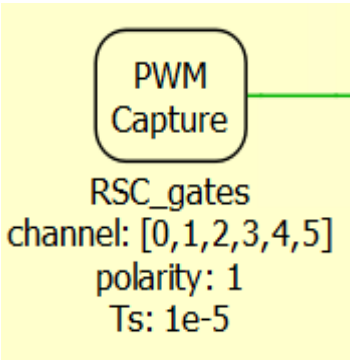

Figure 14: PWM Capture block

Remember to set the analog out limits on the RT-Box 1 to +-10V

Results

The following section demonstrates that the implemented DFIG control functions as intended.

As expected, Figures 17 and 18 show how the RSC can operate the DFIG above (with a positive slip) and below (with a negative slip) synchronous speed. Additionally, Figure 17 demonstrates that the GSC converter maintains a high power factor while maintaining a fixed DC bus voltage, regardless of power flow direction.

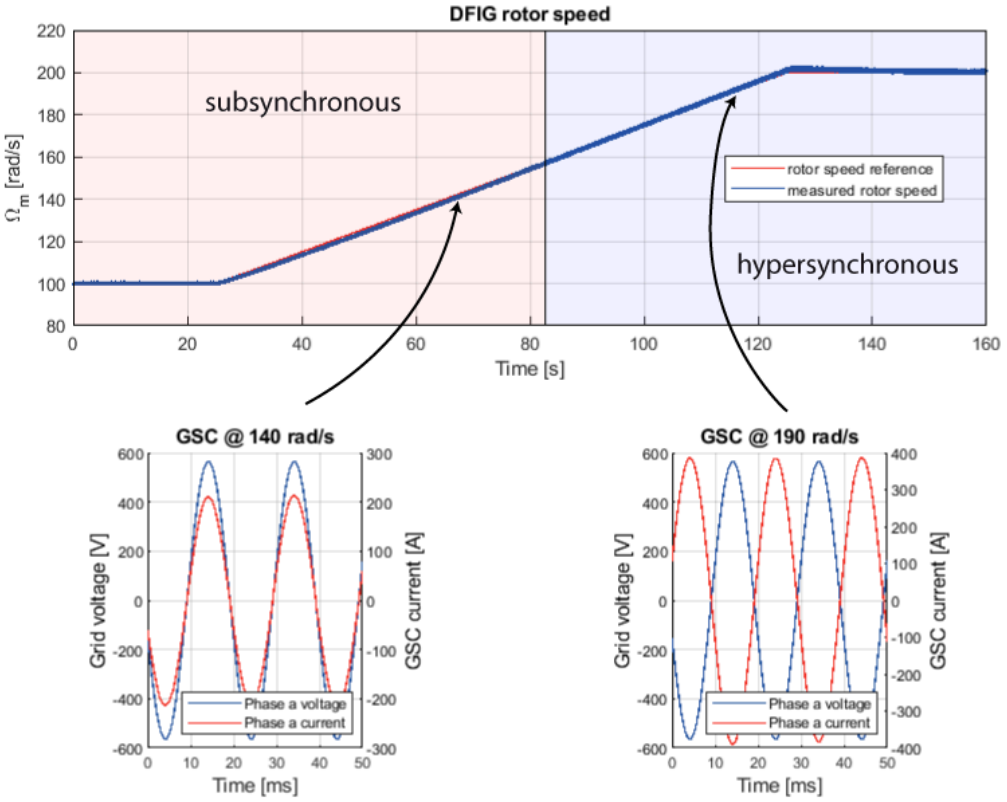

Figure 17: Ramp acceleration of the rotor from 100 rad/s to 200 rad/s

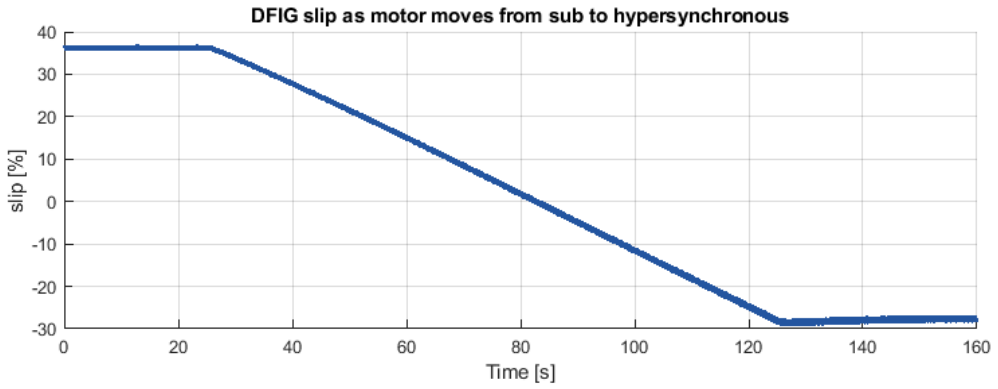

Figure 18: Evolution of slip during the ramp acceleration from Figure 17

As can be seen in Figures 17 and 18, when the DFIG is operating at synchronous speed (~157 rad/s), the rotor slip is equal to 0.

Further, figures 20 and 21 illustrate that the reactive power controller can both sink and generate reactive power according to the setpoint:

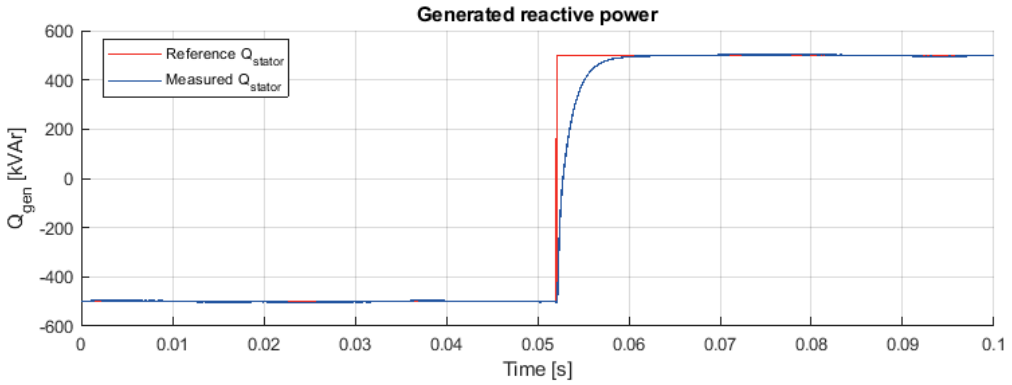

Figure 20: Reactive power step and response from -500 kVAr to 500 kVAr

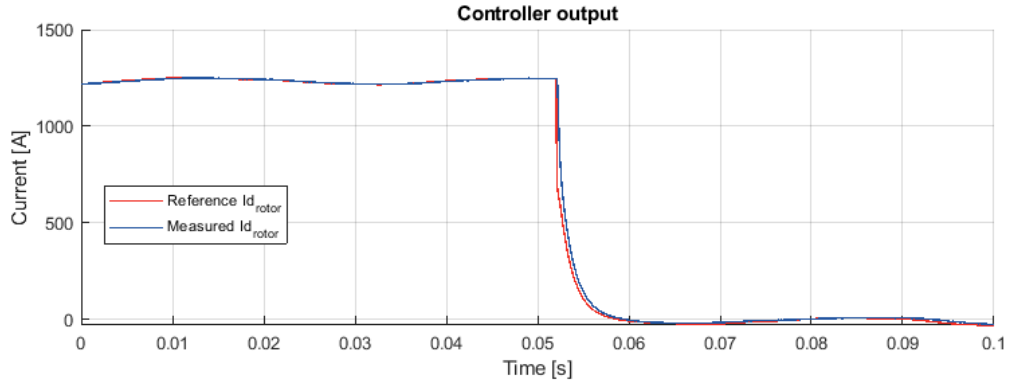

Figure 21: Reactive power controller reference and measured controlled variable for the step from Figure 20

Finally, figures 23 and 24 prove that the MPPT tracking in the model is functioning as expected, tracking the generated power to the peak defined in Figure 15.

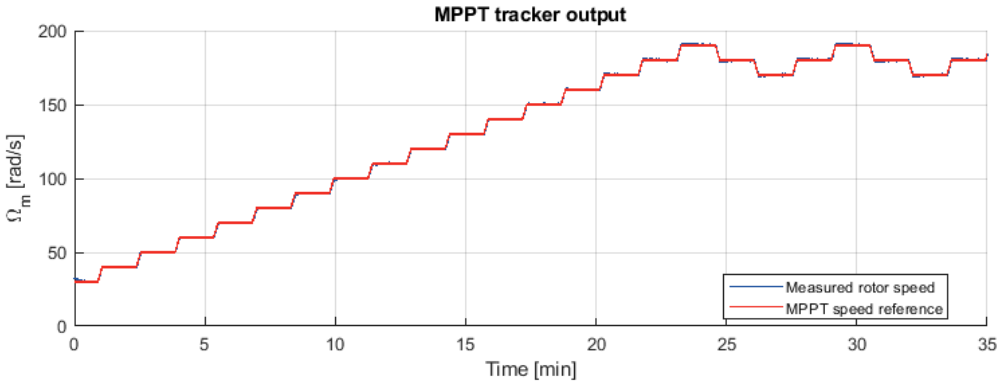

Figure 23: Change in speed reference as the MPPT controller tracks the maximum generated power

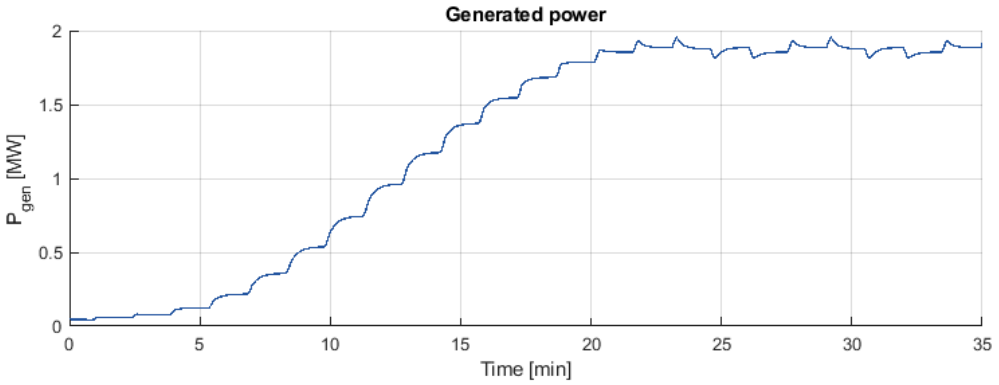

Figure 24: Generated power measured by the MPPT controller with speed reference from Figure 23

References

[1] G. Abad, J. López, M. Rodríguez, L. Marroyo, and G. Iwanski, *Doubly Fed Induction Machine:*
Modeling and Control for Wind Energy Generation, IEEE Press Series on Power Engineering,
Wiley, 2011.

[2] A. Petersson, “Analysis, Modeling and Control of Doubly-Fed Induction Generators for Wind Turbines”, PhD Thesis, Chalmers University of Technology, 2005.